Structural variation in cation-assisted assembly processes of high-nuclearity Mn arsonate and phosphonate wheels

Theresa O. Chimamkpam,[a] Rodolphe Clérac,[b,c] Dmitri Mitcov,[b,c] Brendan Twamley,[a] Munuswamy Venkatesan[d] and Wolfgang Schmitt[a*]

[a] *School of Chemistry and CRANN, Trinity College, The University of Dublin, Dublin 2, Ireland,*
[b] *CNRS, CRPP, UPR 8641, F-33600 Pessac, France.*
[c] *Univ. Bordeaux, CRPP, UPR 8641, F-33600 Pessac, France*
[d] *School of Physics & CRANN, University of Dublin, Trinity College, Dublin 2, Ireland*

Experimental Section

Materials and Instrumentation

Commercially available reagents were bought from Sigma-Aldrich or ABCR and used as received without further purification. Fourier transform infrared spectroscopy (FTIR) data were collected on a PerkinElmer Spectrum 100 FT-IR Spectrometer. Elemental analyses (C, H, and N) were obtained from Microanalysis Lab, School of Chemistry & Chemical Biology, University College Dublin. Thermogravimetric analysis was carried out with a Perkin Elmer Pyriss 1TGA in air at a heating rate of 10 ºC/min in the range 25-900 ºC.

Synthesis of $[K(H_2O)_2 \subset Mn^{III}_8(\mu\text{-}OH)_2(CH_3OH)_2(PhAsO_3)_4(PhAsO_3H)_6(dipic)_4]Cl \cdot 18H_2O \cdot 4CH_3OH$ (1)

$MnCl_2 \cdot 4H_2O$ (0.198 g, 1.0 mmol), $KMnO_4$ (0.040 g, 0.25 mmol), phenyl arsonic acid (0.121 g, 0.60 mmol) and dipicolinic acid (0.084 g, 0.50 mmol) were dissolved under stirring in MeOH (20 mL) at room temperature. The reaction mixture was stirred for 5 hours, filtered and left undisturbed for slow evaporation. Rectangular red brown crystals were obtained within one week. Yield ≈ 64%. Crystals of **1** co-crystallised with un-reacted arsonate ligands and were separated manually. Anal. Calc. for a dried sample, Expected for $C_{94}H_{134}As_{10}ClKMn_8N_4O_{74}$: C % = 30.32, H% = 2.89, N% = 1.61, K% 1.04; Found: C% = 29.63, H% = 2.02, N% = 1.21, K% 1.16.[7] FT-IR (cm^{-1}) ν_{max}: 3356(vbr), 3066(vbr), 1621(vs), 1440(m), 1427(s), 1387(m), 1279(w), 1186(m), 1087(w), 802(vs), 731(w), 684(m).

Synthesis of
$(H_3O)_4[K_2(H_2O)_2\subset Mn_{24}(\mu_3\text{-}O)_4(\mu\text{-}OH)_4(\mu\text{-}CH_3O)_4(H_2O)_8(PhPO_3)_{20}(dipic)_{12}][Mn(H_2O)_6\cdot solv$ (2)

The same synthetic procedure as for **1** was used except that phenyl phosphonic acid (0.095 g, 0.60 mmol) instead of phenyl arsonic acid was used. Reddish brown block crystals were obtained after two weeks. Yield ≈ 48%. Anal. Calc. for a dried sample, containing 30 constitutional H_2O molecules, Expected for $C_{208}H_{256}Mn_{25}P_{20}K_2O_{172}N_{12}$: C% = 32.25, H% = 3.33, N% = 2.17, K% = 1.01; Found: C% = 31.74, H% = 2.70, N% = 2.33, K% 1.25. FT-IR (cm^{-1}) ν_{max}: 3245(vbr), 1622(s), 1487(w), 1390(m), 1281(m), 1135(m), 970(vs), 752(m), 720(m), 679(s).

Magnetic Measurements

The magnetic measurements were carried out with the use of MPMS-XL Quantum Design SQUID magnetometer operating between 1.8 and 400 K with applied dc fields ranging from -7 to 7 T. Measurements were performed on a finely ground polycrystalline sample of **1** and **2**(14.39 and 11.43 mg respectively) sealed in a polypropylene bag (3 × 0.5 × 0.02 cm; 24.09 and 19.69 mg respectively). Ac susceptibility measurements were made with an oscillating field of 3 to 6 Oe with a frequency from 1 to 10000 Hz but no out-of-phase signal was detected above 1.8 K. Prior to the experiments, the field-dependent magnetization was measured at 100 K in order to detect the presence of any bulk ferromagnetic impurities. The samples appeared to be free of any significant ferromagnetic impurities. The magnetic data were corrected for the sample holder and the intrinsic diamagnetic contributions.

X-ray Crystallography

Single crystal X-ray structure determination of the two compounds, were performed at 200(K) on the Bruker SMART Apex diffractometer using a high intensity Cu-Kα source (λ = 1.5418 Å) generated from a micro-focus anode. The omega and phi scans method was used to collect either a full sphere or hemisphere of data for each crystal with a detector to crystal distance of either 5 or 6 cm. The data sets were processed and corrected for Lorentz and polarisation effects using SMART[1] and SAINT-PLUS[2] software. The structures were solved using direct methods with the SHELXTL[3] program package. Data integration, reduction and correction for absorption and polarisation effects were all performed using the Crystalclear-SM 1.4.0 software.[4] Space group determination; structure solution and refinement were obtained using the Crystal structure ver.3.8 and the Bruker SHELXTL[3] software. The

structures were solved using Bruker APEX v2011.8-0 software.[5] All atoms except H atoms were refined anisotropically. Hydrogen atoms (excluding water) were assigned to calculated positions using a riding model with appropriately fixed isotropic thermal parameters. Disordered lattice solvent molecules could not be refined satisfactorily using partial atom occupancies and suitable restraints were handled using the SQUEEZE option in PLATON.[6] Crystal data and details of data collection and refinement of **1** and **2** are summarized in Tables S1-S4

Crystallographic data, CCDC 1428584 & 1428585 can be obtained free of charge from the Cambridge Crystallographic Data Centre via www.ccdc.cam.ac.uk/data_request/cif.

Table S1 - Crystal data and structure refinement parameters for 1.

Empirical formula	$C_{94}H_{134}As_{10}ClKMn_8N_4O_{74}$
Molecular weight/g mol^{-1}	3767.34
Temperature/K	100(2)
Crystal system	monoclinic
Space group	C2/c
a/Å	26.9149(9)
b/Å	31.0829(11)
c/Å	21.2174(7)
α/°	90
β/°	96.4956(18)
γ/°	90
Volume/Å^3	17636.4(10)
Z	4
ρ_{calc}g/cm^3	1.232
F(000)	6400.0
Crystal size/mm^3	0.160 × 0.070 × 0.070
Radiation	CuKα (λ = 1.54178)
2Θ range for data collection/°	4.358 to 120.348
Index ranges	-30 ≤ h ≤ 29, -34 ≤ k ≤ 34, -23 ≤ l ≤ 23
Reflections collected	93912
Independent reflections	13121 [R_{int} = 0.0800, R_{sigma} = 0.0450]
Data/restraints/parameters	13121/340/684
Goodness-of-fit on F^2	1.021
Final R indexes [I ≥ 2σ (I)]	R_1 = 0.0538, wR_2 = 0.1512
Final R indexes [all data]	R_1 = 0.0836, wR_2 = 0.1757
Largest diff. peak/hole / e Å^{-3}	1.17/-0.48

Table S2- Crystal data and structure refinement parameters for 2.

Empirical formula	$C_{208}H_{184}K_2Mn_{25}N_{12}O_{138}P_{20}$
Molecular weight/g mol^{-1}	7747.37
Temperature/K	100(2)
Crystal system	orthorhombic
Space group	Pnn2
a/Å	47.9173(14)
b/Å	13.8095(6)
c/Å	25.5449(8)
α/°	90
β/°	90
γ/°	90
Volume/Å^3	16903.4(10)
Z	2
ρ_{calc}g/cm^3	1.401
μ/mm^{-1}	9.161
F(000)	7166.0
Crystal size/mm^3	0.300 × 0.260 × 0.200
Radiation	CuKα (λ = 1.54178)
2Θ range for data collection/°	3.92 to 134.252
Index ranges	-56 ≤ h ≤ 52, -15 ≤ k ≤ 16, -23 ≤ l ≤ 30
Reflections collected	73910
Independent reflections	25071 [R_{int} = 0.1231, R_{sigma} = 0.1161]
Data/restraints/parameters	25071/3371/1543
Goodness-of-fit on F^2	1.000
Final R indexes [I ≥ 2σ (I)]	R_1 = 0.0804, wR_2 = 0.2036
Final R indexes [all data]	R_1 = 0.1452, wR_2 = 0.2427
Largest diff. peak/hole / e Å^{-3}	0.78/-0.68

Table S3- Selected bond lengths [Å] and bond valence sum for compound 1.

Atom	Bond	Bond distances (Å)	Bond valence sum	Bond valence sum/Assigned oxidation state
Mn(1)	Mn(1)-O(3) Mn(1)-O(4) Mn(1)-O(6) Mn(1)-O(8`) Mn(1)-O(11`) Mn(1)-N(1)	1.953(5) 2.238(4) 2.155(5) 1.899(5) 1.925(4) 2.028(6)	0.593 0.274 0.343 0.686 0.640 0.638	3.174/+3
Mn(2)	Mn(2)-O(10) Mn(2)-O(12) Mn(2)-O(14) Mn(2)-O(16) Mn(2)-O(18) Mn(2)-N(2)	1.941(4) 1.890(5) 2.147(5) 2.255(4) 1.928(5) 2.021(6)	0.612 0.703 0.351 0.262 0.634 0.650	3.212/+3
Mn(3)	Mn(3)-(O5) Mn(3)-O(13) Mn(3)-O(16) Mn(3)-O(19) Mn(3)-O(21) Mn(3)-O(24)	2.223(4) 1.917(4) 2.309(5) 1.927(4) 1.891(4) 1.946 (4)	0.286 0.654 0.226 0.636 0.701 0.604	3.107/+3
Mn(4)	Mn(4)-O(2´) Mn(4)-O(4) Mn(4)-O(9`) Mn(4)-O(22) Mn(4)-O(24) Mn(4)-O(25)	1.911(4) 2.247(5) 1.931(4) 1.911(5) 1.936(4) 2.261(6)	0.664 0.268 0.629 0.664 0.621 0.258	3.104/+3

Table S4 – Selected bond lengths [Å] and bond valence sum for compound 2.

Atom	Bond	Bond distances (Å)	Bond Valence	Bond valence sum
Mn(1)	Mn(1)-O(1`) Mn(1)-O(3) Mn(1)-O(4) Mn(1)-O(31) Mn(1)-O(33) Mn(1)-N(1)	1.880(12) 1.891(12) 1.857(12) 2.163(6) 2.225(6) 1.974(6)	0.700 0.679 0.745 0.330 0.279 0.738	3.471
Mn(2)	Mn(2)-O(2) Mn(2)-O(5) Mn(2)-O(7) Mn(2)-O(33) Mn(2)-O(55) Mn(2)-O(56)	1.910(11) 1.918(11) 1.875(13) 2.319(7) 1.859(11) 2.221(15)	0.667 0.652 0.733 0.220 0.765 0.288	3.325
Mn(3)	Mn(3)-(O8) Mn(3)-O(34) Mn(3)-O(40) Mn(3)-O(55) Mn(3)-O(57) Mn(3)-O(58)	1.888(12) 2.207(7) 2.246(8) 1.951(12) 1.887(10) 1.907(12)	0.707 0.298 0.268 0.597 0.709 0.672	3.251
Mn(4)	Mn(4)-O(6) Mn(4)-O(10) Mn(4)-O(35) Mn(4)-O(37) Mn(4)-O(57) Mn(4)-N(2´)	1.914(11) 1.913(12) 2.234(6) 2.160(5) 1.894(11) 1.984(6)	0.659 0.661 0.277 0.339 0.696 0.719	3.351
Mn(5)	Mn(5)-O(11) Mn(5)-O(14) Mn(5)-O(39) Mn(5)-O(57) Mn(5)-O(58) Mn(5)-O(59)	1.956(11) 1.911(11) 2.319(7) 1.891(11) 1.870(11) 2.244(14)	0.589 0.665 0.220 0.702 0.743 0.270	3.189
Mn(6)	Mn(6)-O(12) Mn(6)-O(13) Mn(6)-O(16) Mn(6)-N(3) Mn(6)-O(39) Mn(6)-O(41)	1.877(12) 1.851(13) 1.882(12) 1.978(7) 2.186(7) 2.207(8)	0.706 0.755 0.696 0.544 0.310 0.293	3.304
Mn(7)	Mn(7)-O(15) Mn(7)-O(18) Mn(7)-O(20) Mn(7)-N(4) Mn(7)- O(43) Mn(7)-O(45)	1.878(11) 1.865(13) 1.894(11) 1.980(6) 2.185(6) 2.224(6)	0.706 0.727 0.676 0.727 0.311 0.280	3.453

Mn(8)	Mn(8)-O(17) Mn(8)-O(19) Mn(8)-O(45) Mn(8)-O(60) Mn(8)-O(61) Mn(8)-O(62)	1.892(12) 1.878(11) 2.272(6) 2.169(12) 1.908(11) 1.895(11)	0.700 0.727 0.250 0.331 0.670 0.694	3.372
Mn(9)	Mn(9)-O(25) Mn(9)-O(46) Mn(9)-O(52) Mn(9)-O(61) Mn(9)-O(62) Mn(9)-O(63)	1.901(12) 2.262(7) 2.195(9) 1.925(12) 1.910(11) 1.935(13)	0.683 0.257 0.308 0.640 0.667 0.623	3.178
Mn(10)	Mn(10)-O(21) Mn(10)-O(23) Mn(10)-O(47) Mn(10)-O(49) Mn(10)-N(5) Mn(10)-O(62)	1.903(10) 1.904(11) 2.193(9) 2.214(9) 2.005(7) 1.910(11)	0.679 0.677 0.310 0.292 0.679 0.667	3.304
Mn(11)	Mn(11)-O(22) Mn(11)-O(26) Mn(11)-O(28) Mn(11)-O(51) Mn(11)-O(63) Mn(11)-O(64)	1.960(17) 1.880(15) 1.916(13) 2.218(8) 1.871(11) 2.294(17)	0.582 0.723 0.656 0.289 0.741 0.236	3.227
Mn(12)	Mn(12)-O(24) Mn(12)-O(29`) Mn(12)-O(30) Mn(12)-N(6) Mn(12)-O(51) Mn(12)-O(53)	1.886(13) 1.900(15) 1.83(2) 1.919(11) 2.205(8) 2.158(10)	0.687 0.658 0.808 0.833 0.294 0.332	3.612
Mn(13)	Mn1(3)-O(65) Mn(13)-O(66) Mn(13)-O(67) Mn1(3)-O(67A) Mn(13)-O(68) Mn(13)-O(68A)	2.1745 2.1747 2.1748 2.1750 2.1745 2.1743	0.354 0.354 0.353 0.353 0.354 0.354	2.122

Table S5 – Bond valence sum calculations for the terminal O atoms in 2.

Atom	**BVS**	**Assignment**
Mn(2)-O(56)	0.329	H_2O
Mn(5)-O(59)	0.266	H_2O
Mn(8)-O(60)	0.328	H_2O
Mn(11)-O(64)	0.301	H_2O

An oxygen BVS in the ~1.8-2.0, ~1.0-1.2, and ~0.2-0.4 ranges is indicative of non-, single- and double protonation, respectively.[8,9]

Table S6 – Bond valence sum calculations for O(62) bridging between Mn(8), Mn(9) and Mn(10).

Atom	Bond distance	BV	BVS	Assignment
Mn(10)-O(62)	1.910(11)	0.667	2.028	μ_3-O^{2-}
Mn(9)-O(62)	1.910(11)	0.667		
Mn(8)-O(62)	1.895(11)	0.694		

An oxygen BVS in the ~1.8-2.0, ~1.0-1.2, and ~0.2-0.4 ranges is indicative of non-, single- and double protonation, respectively.[8, 9]

Table S7 – Bond valence sum calculations for O(57) bridging between Mn(3), Mn(4) and Mn(5).

Atom	Bond distance	BV	BVS	Assignment
Mn(3)-O(57)	1.887(10)	0.709	2.107	μ_3-O^{2-}
Mn(4)-O(57)	1.894(11)	0.696		
Mn(5)-O(57)	1.891(11)	0.702		

An oxygen BVS in the ~1.8-2.0, ~1.0-1.2, and ~0.2-0.4 ranges is indicative of non-, single- and double protonation, respectively.[8, 9]

Table S8 – Bond valence sum calculations for Mn-OH bonds (O(55) and O(63) bridging between (Mn(2)/Mn(3)) and (Mn(9)/Mn(11) respectively).

Atom	Bond length	BV	BVS	Assignment
Mn(2)-O(55)	1.859(11)	0.765	1.362	μ-OH^-
Mn(3)-O(55)	1.951(12)	0.597		
Mn(9)-O(63)	1.935(13)	0.623	1.373	μ-OH^-
Mn(11)-O(63)	1.871(11)	0.741		

An oxygen BVS in the ~1.8-2.0, ~1.0-1.2, and ~0.2-0.4 ranges is indicative of non-, single- and double protonation, respectively.[8, 9]

a)

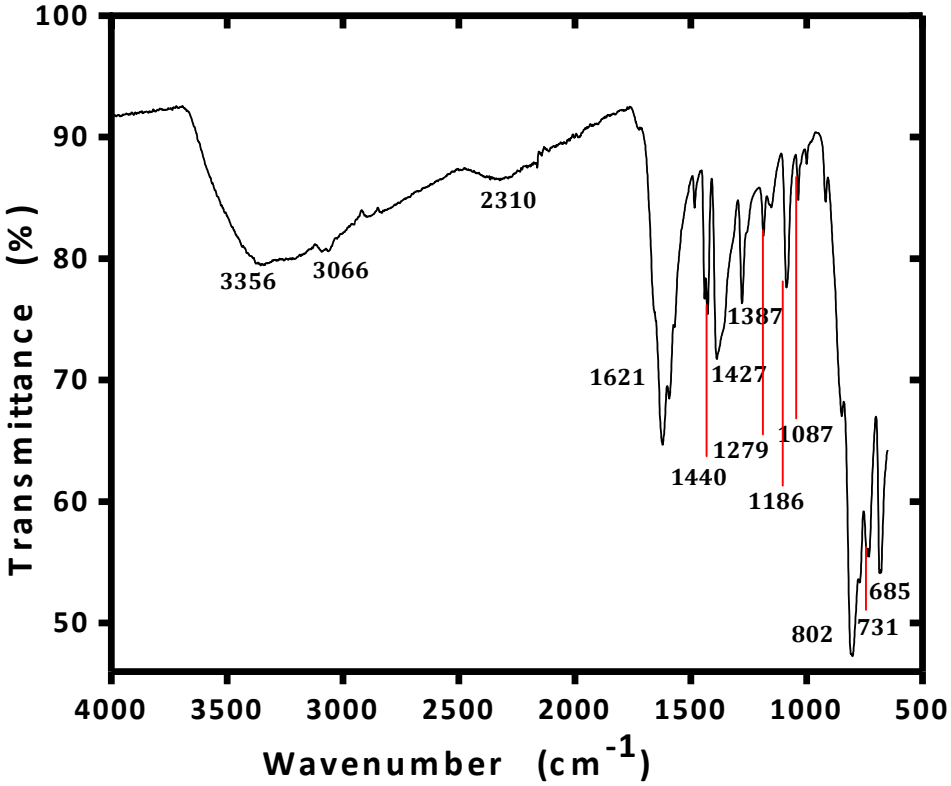

b)

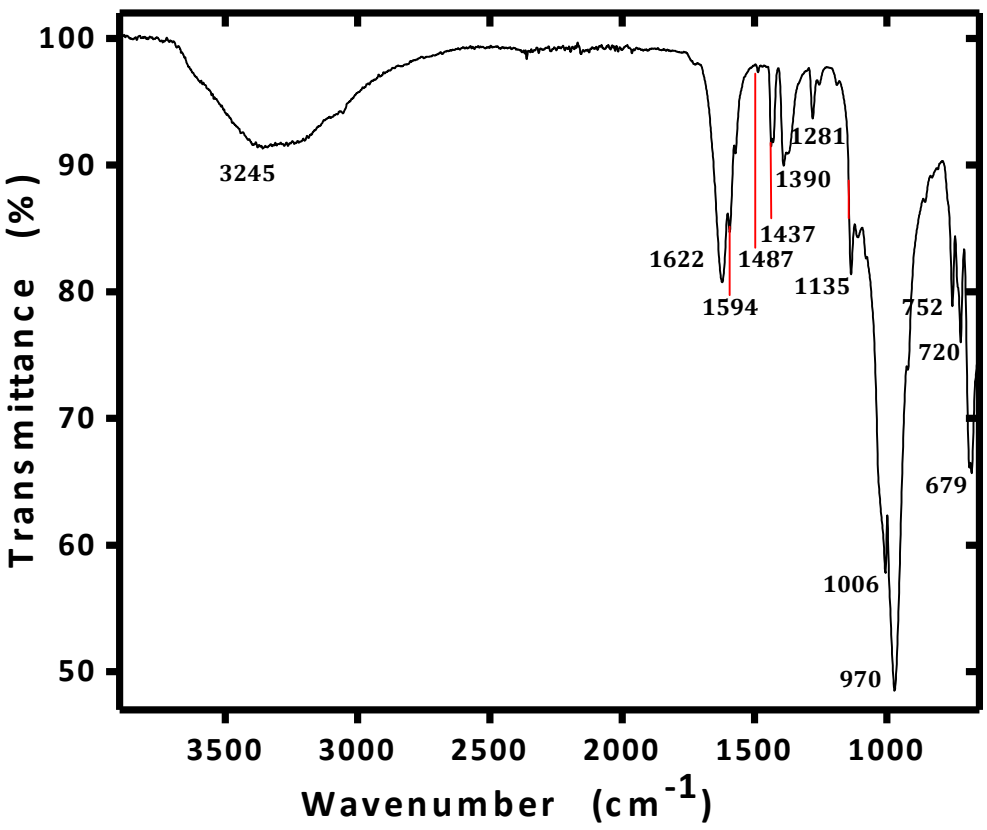

Fig. S1- Infrared spectra recorded at room temperature for compounds **1** (a) and **2** (b).

a)

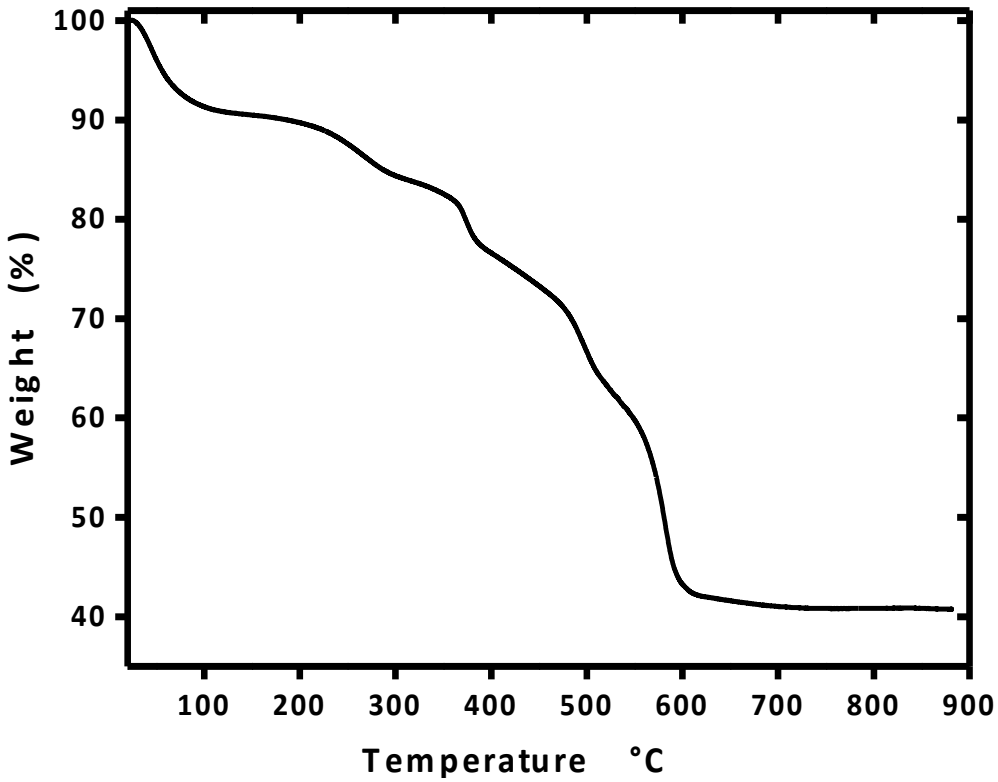

b)

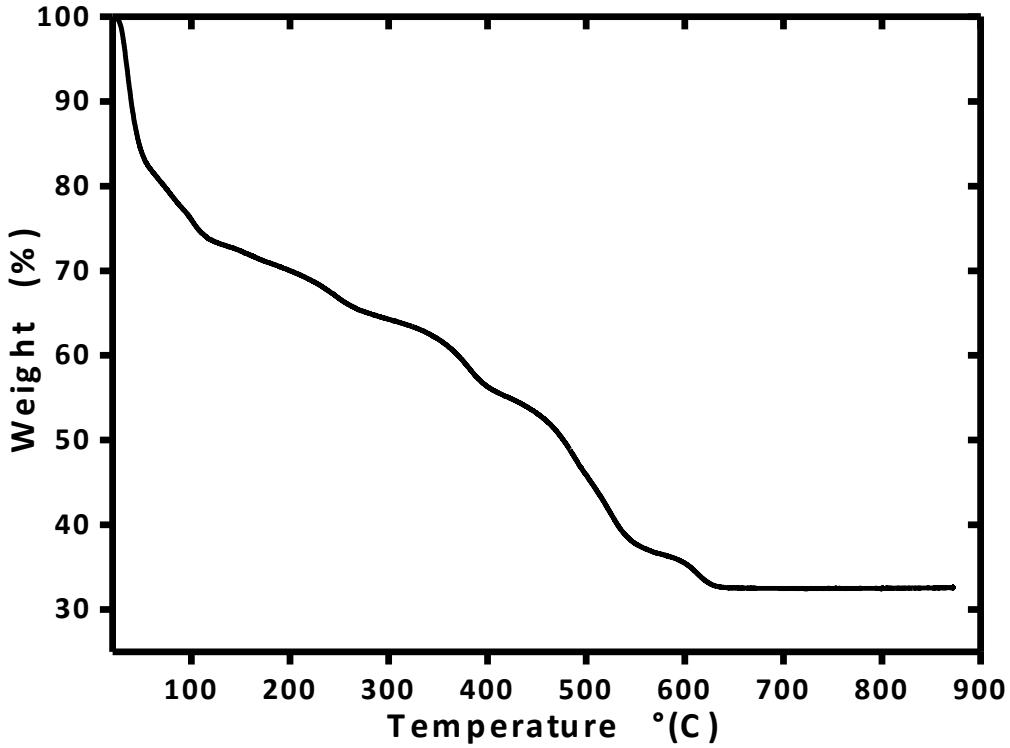

Fig. S2 – TGA for compounds **1** (a) and **2** (b).

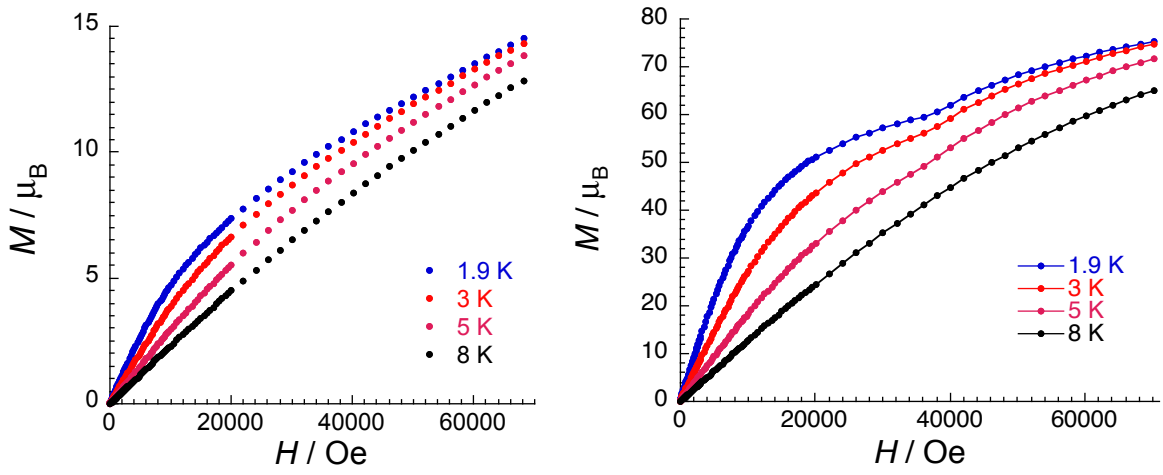

Fig. S3 - Field dependence of magnetisation for **1** (left) and for **2** (right) at 1.9, 3, 5 and 8 K between 0 and 70 kOe.

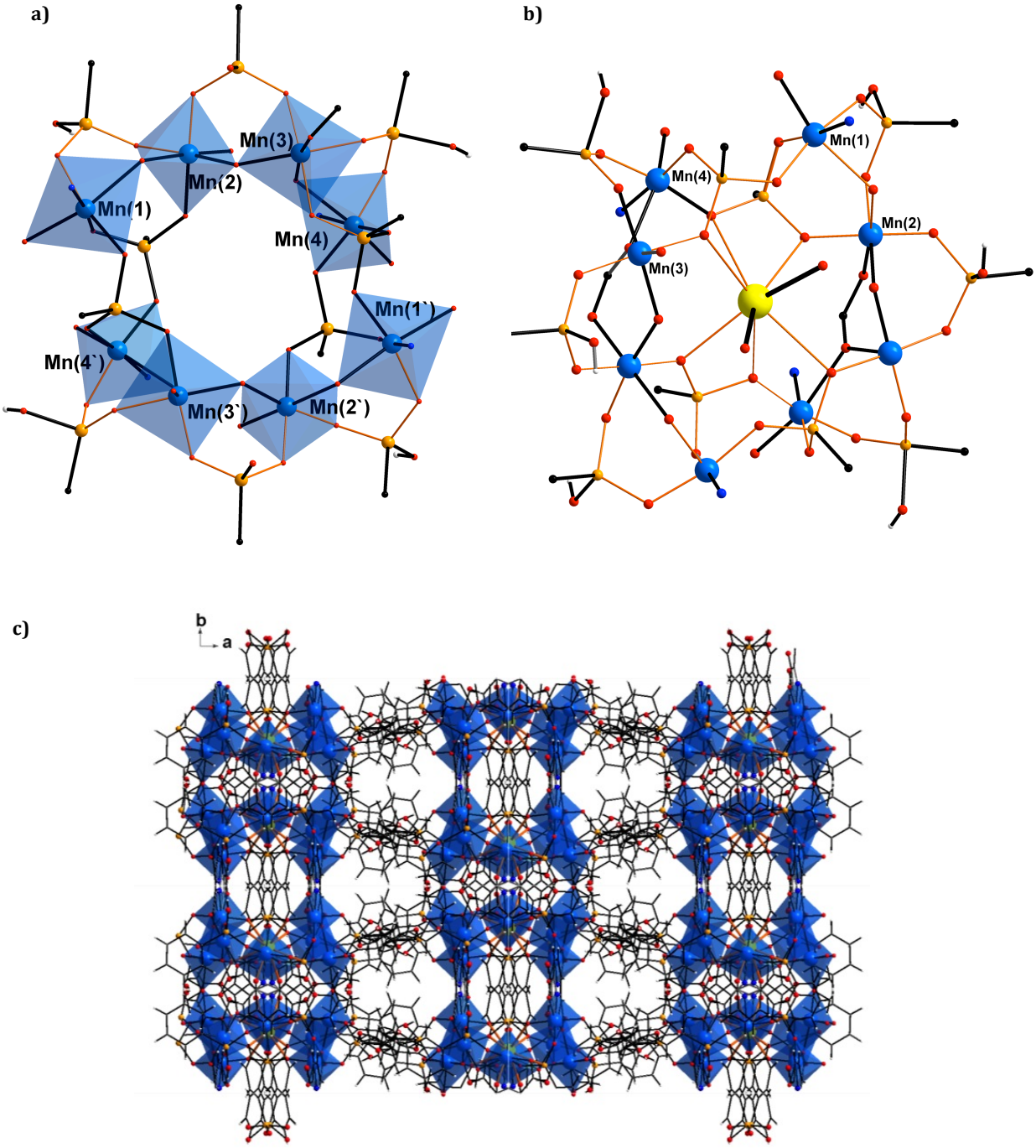

Fig. S4 - a) Polyhedral representation of the $\{Mn_8\}$ core highlighting the binding modes of the outer arsonate functionalities to Mn ions, b) highlighting the binding modes of the inner arsonate functionalities to Mn and K, c) packing arrangement of **1** viewed in the direction of the crystallographic *c*-axis. All crystallization solvent molecules and counter ion have been omitted for clarity.

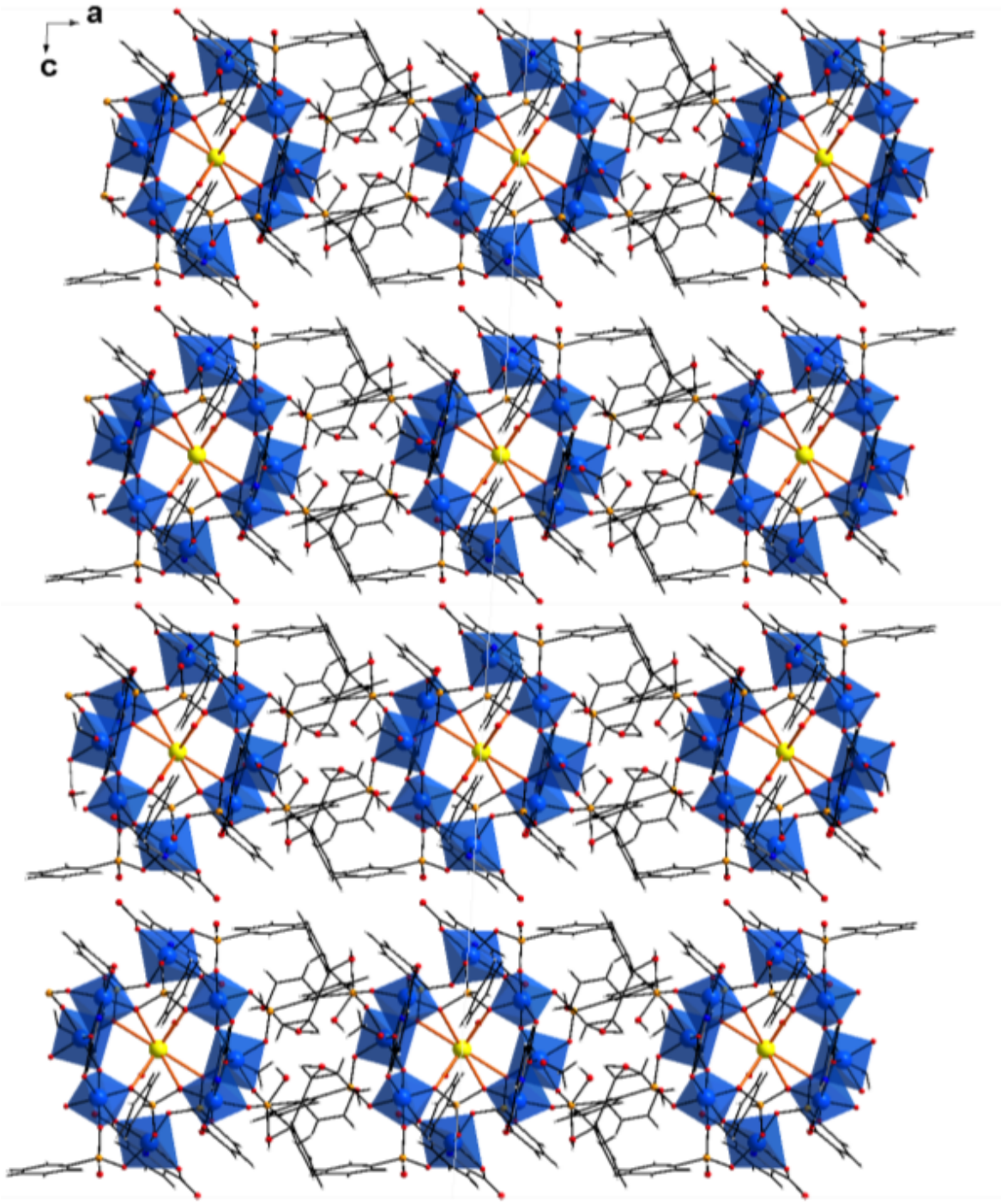

Fig. S5 - Packing arrangement of **1** viewed in the direction of the crystallographic *b*-axis. Colour code: Mn blue, As orange, K yellow, N dark blue, C black.

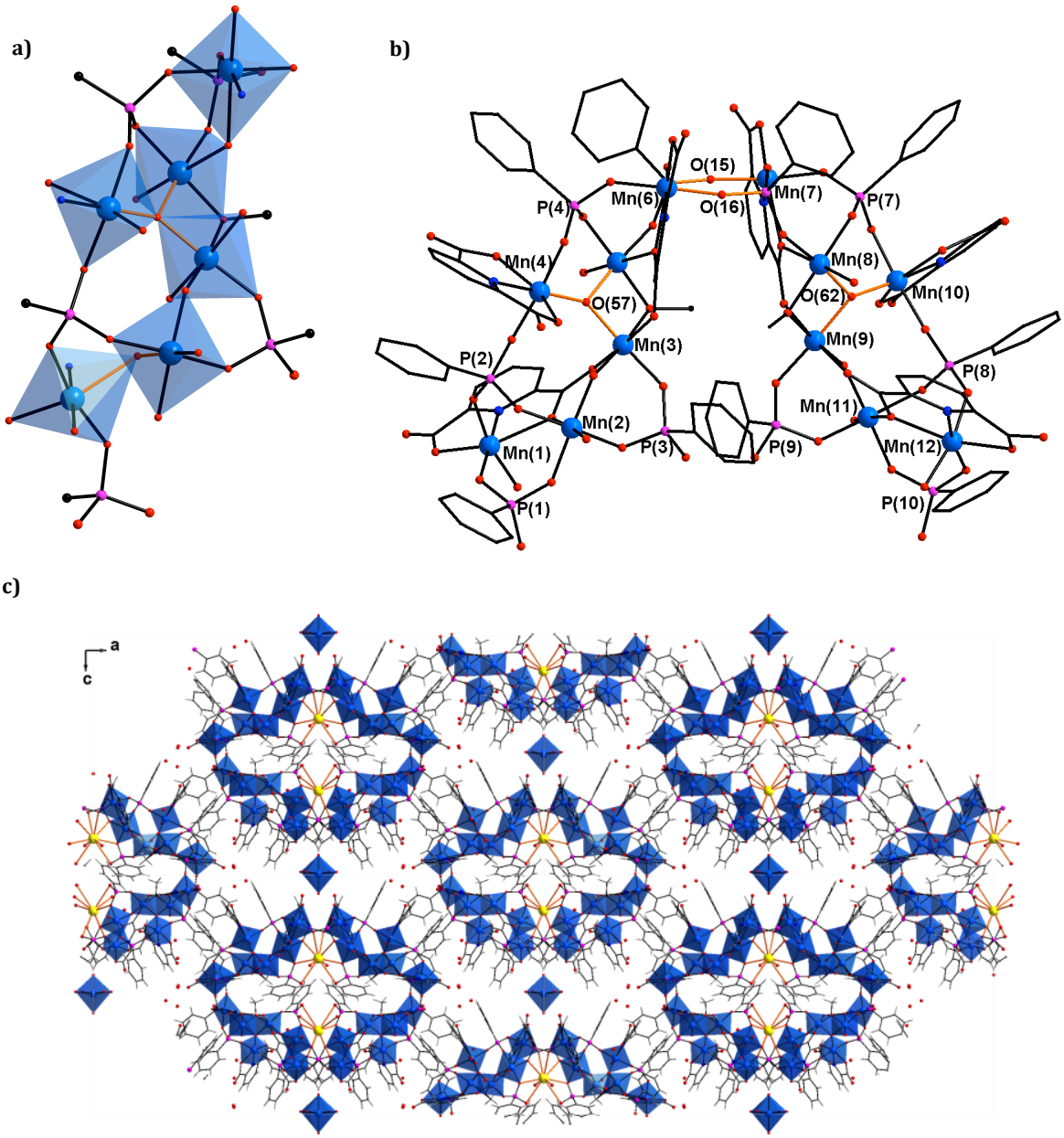

Fig. S6 – a) -{Mn_6} unit in **2,** b) - the symmetry-independent {Mn_{12}} units in **2** highlighting the bridging O atoms, c) packing arrangement of compound **2** viewed in the direction of the crystallographic *b*-axis. The phenyl rings of the ligands in the {Mn_6} unit have been omitted for clarity.

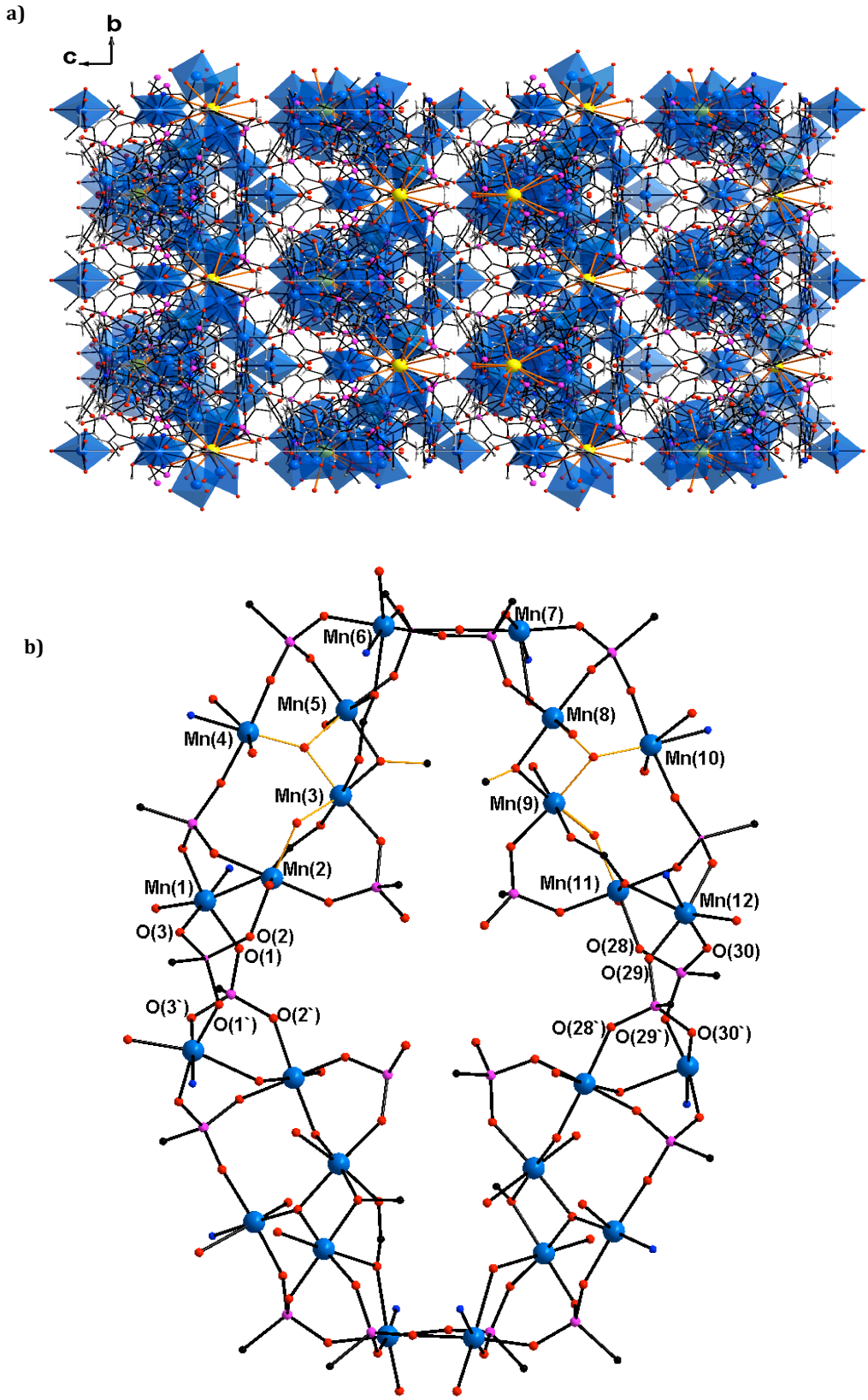

Fig. S7 – a) The packing arrangement of compound **2** viewed in the direction of the crystallographic *a*-axis, b) core structure of **2** showing the connection of the two $\{Mn_{12}\}$ units through O donors of the phosphonate ligands. Colour code: Mn blue, N dark blue, C black, P pink, K yellow, O red (the phenyl rings of the organo-phoshonate ligands and organic residues of the dipicolinate ligands and H atoms have been omitted for clarity).

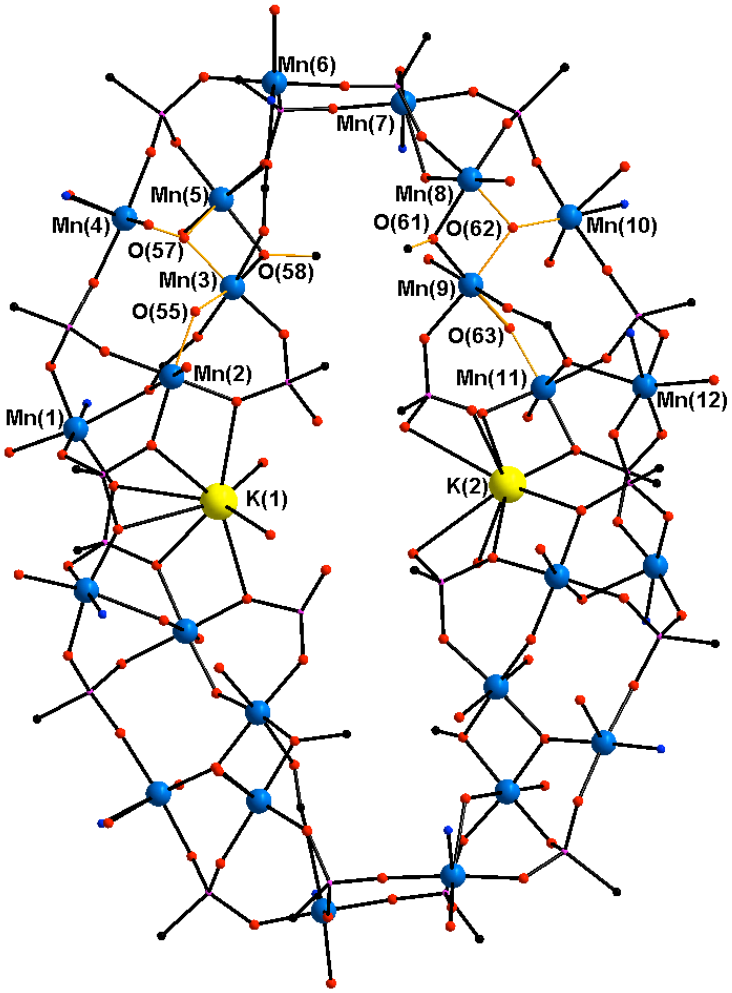

Fig. S8 – The core structure of **2** showing the connection of the two $\{Mn_{12}\}$ units through the central K^+ ions. Colour code as above (the phenyl rings of the organo-phoshonate ligands and organic residues of the dipicolinate ligands and H atoms have been omitted for clarity).

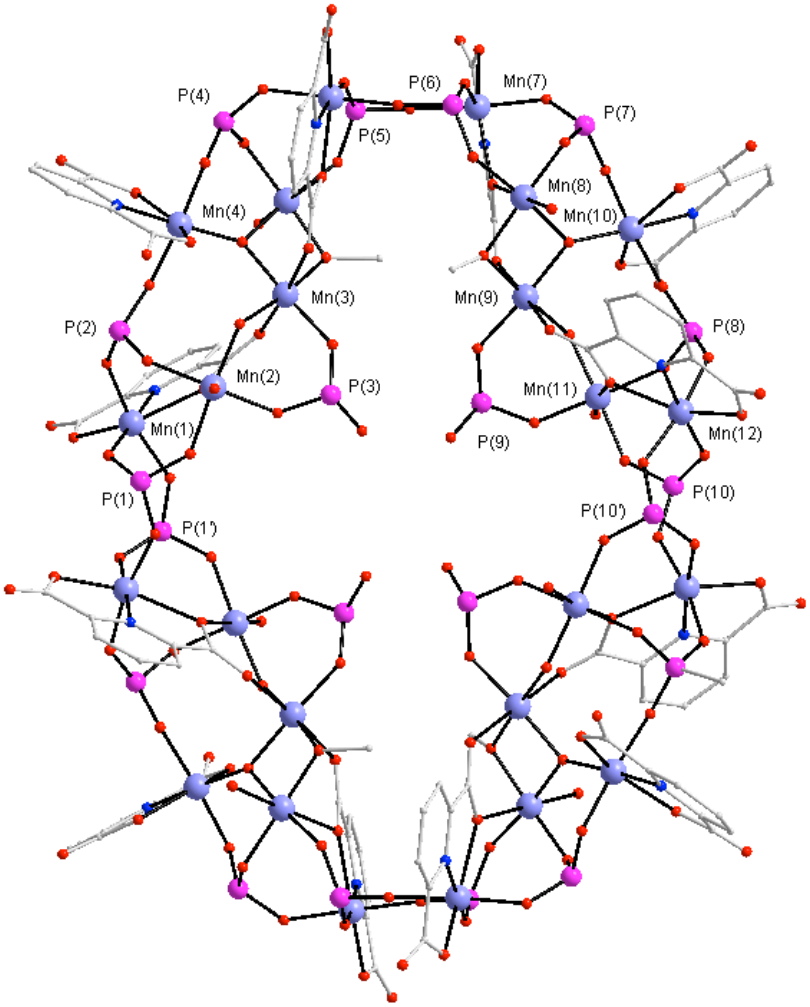

Fig. S9 – The core structure of **2** highlighting the bridging modes of the organic ligands (H atoms, K atoms and C atoms of the phosphonates have been omitted for clarity).

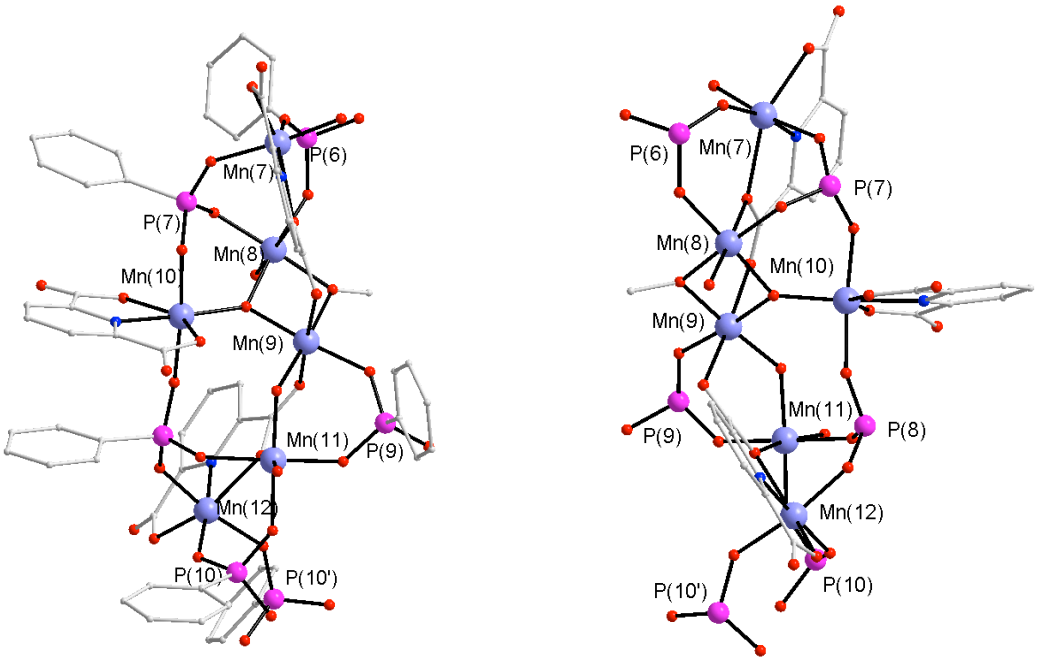

Fig. S10 – Structural motif in **2** highlighting the bridging modes of the organic ligands (H atoms, K atoms have been omitted for clarity; in the representation on the left C atoms of the phosphonates have additionally been omitted).

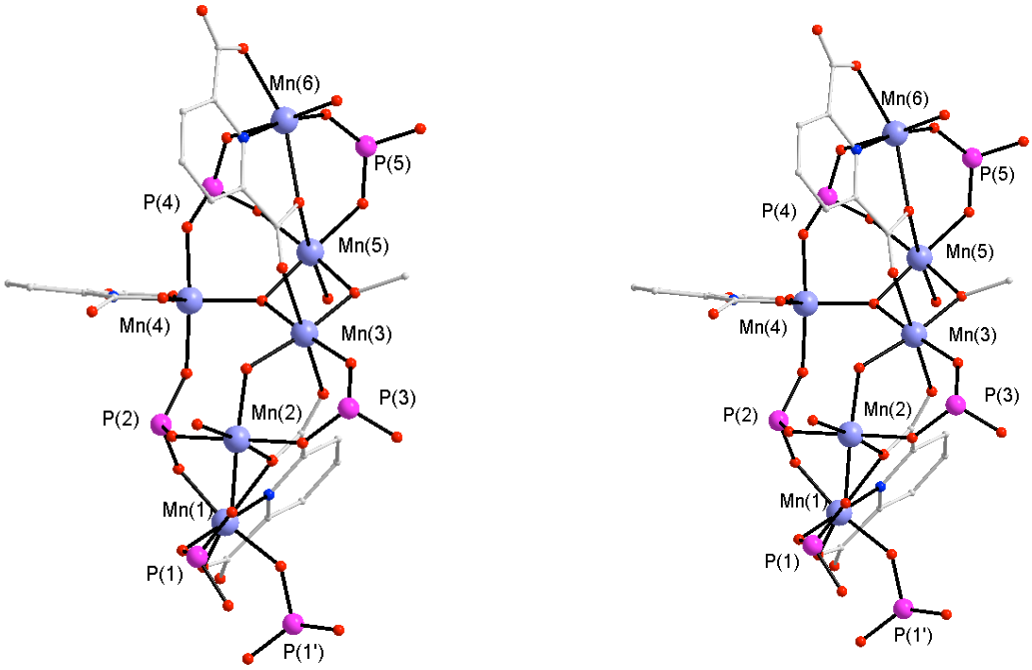

Fig. S11 – Structural motif in **2** highlighting the bridging modes of the organic ligands (H atoms, K atoms have been omitted for clarity; in the representation on the left C atoms of the phosphonates have additionally been omitted).

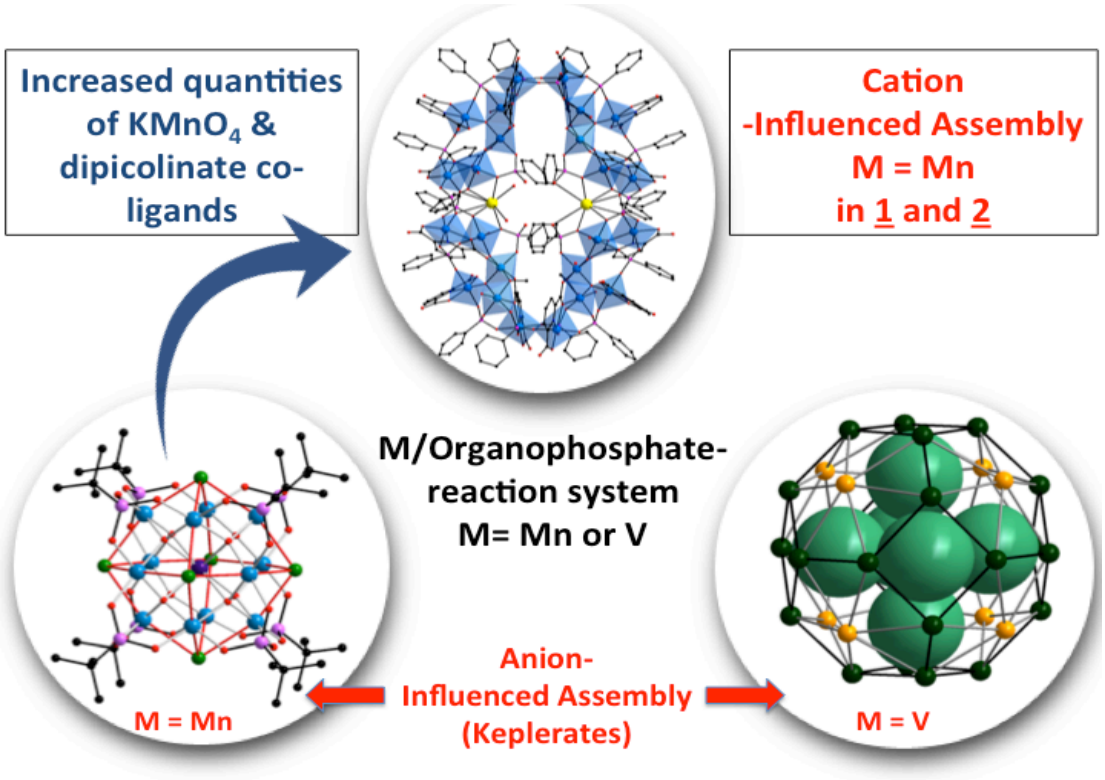

Fig. S12 – Cation- and anion-influenced assembly of polynuclear Mn complexes and polyoxovanadates in phosphonate-stabilised reaction systems (compare refs. 7 & 8 in the main text).

References

1. Bruker SMART, Version 5.629, 1997-2003, Bruker-Axs Inc.
2. Bruker Saint-Plus, Version 6.22, 1997-2003, Bruker-Axs Inc.
3. G. M. Sheldrick, Version 5.1, 1999, Bruker Axs-Inc.
4. Rigaku Americas Corporation, Crystalclear-SM 1.4.0 software, 9009 New Trails Drive, The Woodlands, TX 77381, United States.
5. Software Reference Manual, version 5.625; Bruker Analytical X-Ray Systems Inc.: Madison, WI, 2001.
6. A. L. Spek, *J.App. Cryst.(Wiley-Blackwell)*, 2003, **36**, 7.
7. The CHN data for **1** deviate from theory due to crystal lattice solvents.
8. T.C. Stamatatos, V. Nastopoulos, A.J. Tasiopoulos, E.E. Moushi, W. Wernsdorfer, G. Christou and S. P. Perlepes, *Inorg. Chem.*, 2008, **47**, 10081.
9. C. Lampropoulos, C. Koo, S. O. Hill, K. Abboud and G. Christou, *Inorg. Chem.*, 2008, **47**, 11180.